

Article

Search Improvement Process-Chaotic Optimization-Particle Swarm Optimization-Elite Retention Strategy and Improved Combined Cooling-Heating-Power Strategy Based Two-Time Scale Multi-Objective Optimization Model for Stand-Alone Microgrid Operation

Fei Wang ^{1,2} , Lidong Zhou ¹, Hui Ren ^{1,*} and Xiaoli Liu ³

¹ State Key Laboratory of Alternate Electrical Power System with Renewable Energy Sources, North China Electric Power University, Baoding 071003, China; feiwang@ncepu.edu.cn (F.W.); zhoulidong_ncepu@sina.com (L.Z.)

² Department of Electrical and Computer Engineering, University of Illinois at Urbana-Champaign, Urbana 61801, IL, USA

³ Shuozhou Power Company of State Grid Shanxi Electric Power Company, Shuozhou 036000, China; ncepulxl@sina.com

* Correspondence: hren@ncepu.edu.cn; Tel.: +86-139-3328-5267

Received: 18 October 2017; Accepted: 10 November 2017; Published: 23 November 2017

Abstract: The optimal dispatching model for a stand-alone microgrid (MG) is of great importance to its operation reliability and economy. This paper aims at addressing the difficulties in improving the operational economy and maintaining the power balance under uncertain load demand and renewable generation, which could be even worse in such abnormal conditions as storms or abnormally low or high temperatures. A new two-time scale multi-objective optimization model, including day-ahead cursory scheduling and real-time scheduling for finer adjustments, is proposed to optimize the operational cost, load shedding compensation and environmental benefit of stand-alone MG through controllable load (CL) and multi-distributed generations (DGs). The main novelty of the proposed model is that the synergetic response of CL and energy storage system (ESS) in real-time scheduling offset the operation uncertainty quickly. And the improved dispatch strategy for combined cooling-heating-power (CCHP) enhanced the system economy while the comfort is guaranteed. An improved algorithm, Search Improvement Process-Chaotic Optimization-Particle Swarm Optimization-Elite Retention Strategy (SIP-CO-PSO-ERS) algorithm with strong searching capability and fast convergence speed, was presented to deal with the problem brought by the increased errors between actual renewable generation and load and prior predictions. Four typical scenarios are designed according to the combinations of day types (work day or weekend) and weather categories (sunny or rainy) to verify the performance of the presented dispatch strategy. The simulation results show that the proposed two-time scale model and SIP-CO-PSO-ERS algorithm exhibit better performance in adaptability, convergence speed and search ability than conventional methods for the stand-alone MG's operation.

Keywords: stand-alone MG; SIP-CO-PSO-ERS; two-time scale optimized model; improved CCHP dispatch strategy; multi-scenario; economic dispatch

1. Introduction

Owing to the great pressure of the global energy crisis and environmental pollution [1], much effort has been devoted to integrating different kinds of distributed generations (DGs) into microgrids (MGs) in order to reduce carbon emissions and improve power quality [2]. MGs could operate in grid-connected or islanded mode, managing all kinds of DGs effectively [3]. This is an ideal way to realize local coordination control and optimized operation of multi-DGs, including micro-gas turbines (MTs), diesel engines (DEs), fuel cells (FCs), photovoltaics (PVs), wind turbines (WTs), small hydropower and some energy storage devices such as flywheels, super capacitors and accumulators [4]. Most of the existing MGs are designed to work primarily under on-grid mode, excluding emergency situations [5]. However, the impact of hybrid renewable energy sources (HRES) to power system should be paid much attention. Researches such as the unsymmetrical faults [6], improvement of transient stability [7], ground fault current [8] were conducted for MG and they are beneficial to the application of renewable energies. On the other hand, more and more attention is drawn to study the stand-alone MG for its capability to supply power economically in some other particular applications, such as MGs for islands or remote areas without power grids [9,10].

For a small but important power system like MG, the problems of voltage balance [11], fault current limit and power system stability are also very important. All in all, the power quality [12] must be guaranteed through a series means such as storage coordination [13], dynamic control [14] or demand response (DR) [15]. Fortunately, all these operation requirements could be included into the optimized operation model as constraints. In order to take full advantages of stand-alone MGs and promote their popularization, researchers around the world have devoted momentous efforts to the optimal operation of stand-alone MGs [16]. However, the uncertainty of renewable power generation because of weather conditions [17–19] and load demand challenges the economic operation a lot. Because of the uncertainty, the predicted data of renewable energy and demand is subject to errors, which negatively affect the optimized generation schedules and operation plans [20,21]. As a result, the economic operation cannot be realized and even the power balance would be broken in extreme conditions such as storms, abnormally high or low temperatures, or part damage of distribution facilities.

To mitigate the impact of uncertainty on optimized operation, energy storage devices were introduced to ensure the safety and reliability of the MG with consideration of their lifetime characteristics [22]. However, the advantage of fast responses for batteries was not used to its full extent and the environmental benefit was not included in the optimization objective. Secondly, the stochastic scheduling method was applied in the MG's optimized operation to decrease the unfavorable effects brought by the uncertainty [23–25]. To a certain degree, the impacts of uncertainty were impaired by transferring the optimal operation into a deterministic optimization problem with a large number of stochastic scenarios. However, the fundamental issue of uncertainty was not resolved because the stochastic method merely dealt with the problem by considering more scenarios while no one could take all scenarios into account due to the complexity of the environment. Another trouble was that the computed burden increased accordingly. Thirdly, with the development of DR, the demand side has been proved an effective tool to improve system reliability and maintain power balance by responding to the dispatch information [26–28]. The applications of DR strategies may help to settle the intermittency of renewable resources by devoting to the balance between energy supply and demand, thus minimizing the operation costs and providing a more reliable grid management [29]. Although DR was considered in studies such as [30–32], the expense for DR was not taken into account and the constraints for DR were not described in the optimized model.

To address these problems and realize the optimized operation of stand-alone MG, this paper establishes a multi-objective optimized model for a stand-alone MG, consisting of PV, WT, FC, DE, MT and an energy storage system (ESS) based on the coordinated operation among sources-load-ESS and an improved dispatch strategy of the MT's CCHP operation mode. It should be pointed that multi-types of micro sources and ESS are considered at the same time so as to improve the stability

and flexibility of stand-alone MG by providing various choices to satisfy the power balance and coping with emergency circumstances. And the installation cost increase of this structure is following therefore. Controllable load (CL) is taken into account as DR resources to improve the reliability. The optimized model is divided into two-time scales in order to deal with the uncertainty of load demand and renewable power generation. The first time scale model is day-ahead optimization, which is to seek a global optimal solution for all the generation resources, CL and ESS, based on the day-ahead predicted data. The renewable integration could be further optimized if storage systems are coupled with DR in order to enlarge load-shifting capacity [33,34]. Therefore, the coordinating operation of ESS and CL are introduced into the second time scale model, called real-time optimization, to adjust the optimized schedule considering the real-time weather condition and demand based on the day-ahead scheduling.

In terms of the optimization solution, various algorithms are developed recently, such as basic particle swarm optimization (PSO) [35], ϵ -constraint method [36] and non-dominated sorting genetic algorithm II (NSGA-II) [37]. All these algorithms achieved relatively good result in the setting of MGs and models. However, the performance needs to be further studied when it comes to different scenarios. PSO is a stochastic and population-based evolutionary algorithm and has gained popularity in the optimized operation of MGs due to its superiorities of having few constraints on fitness function, simple principle, easy coding and rapid convergence speed [38]. However, when major fluctuations occur in the base data of optimized model resulting from different scenarios during stand-alone MG's optimized operation, two problems would appear in PSO algorithm: (i) the local and global search ability is not good enough to find an excellent solution in a relatively short time; (ii) the premature phenomenon would occur due to the loss of population diversity in the later iterations. Moreover, conditions could be worse especially for the model with complex variables and intricate scenarios [39]. Chaotic optimization (CO) has a strong local search capability profiting from the characteristics of randomness, ergodicity and inherent regularity [40] which would be effective to the optimization problem with many variables and the nature of chaos could also decrease the impact that comes from renewable energy or load uncertainty. In addition, an adequate elite retention strategy (ERS) could further improve the solution quality, as well as the convergence speed, even under the inconstant conditions [41]. In order to solve the problems of poor search ability and premature in PSO, this paper introduces a dual-step modification (search improvement process and CO) and ERS into PSO to present a Search Improvement Process-Chaotic Optimization-Particle Swarm Optimization-Elite Retention Strategy (SIP-CO-PSO-ERS). SIP-CO-PSO-ERS was applied to solve the day-ahead scheduling model, while linear programming was used to deal with the real-time scheduling model due to the simplicity of its model which contains fewer decision variables and constraints.

The main contributions of this paper can be summarized as follows:

- A new two-time scale multi-objective optimization model which aims to optimize the operation cost, load cut compensation and environmental benefit of stand-alone MGs that consists of electric, thermal and cooling energy styles based on CL and multi-DGs; the synergetic response of CL and ESS (battery in this paper) in real-time scheduling offsets the operation uncertainty quickly, and the improved dispatch strategy for CCHP enhances the system economy, guaranteeing comfort feel;
- A dual-step modification and ERS are introduced into PSO to present SIP-CO-PSO-ERS, which has a strong search capability and fast convergence speed; four typical scenarios are designed according to diverse situations to verify the adaptation of SIP-CO-PSO-ERS and proposed optimized model.

This paper focuses on the achievement of the presented points and is organized as follows. Section 2 gives descriptions of the two-time scale model. Section 3 gives a detail explanation of the proposed SIP-CO-PSO-ERS method. Simulation is given in Section 4 to illustrate the advantages and validity of the proposed algorithm and model. Section 5 gives a conclusion.

2. Optimization Model

2.1. The CCHP Model and Improved Dispatch Strategy

2.1.1. The CCHP Model of MT

Generally, the efficiency of MTs' working in electricity generation is 30% with full load, or 10~15% with half load. It is very inefficient, letting much heat energy go to waste. Actually, the efficiency could increase to more than 80% if the remaining heat energy is reused by CCHP operation mode [42]. CCHP is composed of a generation module and a heat recovery module, and the latter is further split into an absorption chiller (APC) and a heat-exchanging system (HES). The generation, APC and HES modules export electricity, cold and heat energy, respectively. The structure is shown in Figure 1.

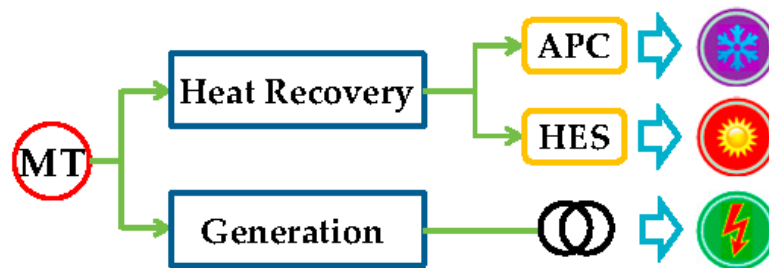


Figure 1. The structure of MT's CCHP operation mode.

The cost model adopted in this paper for MT is expressed by (1) and the mathematical description of heat recovery module is expressed by Equations (2)–(4):

$$C_{MT} = C_{nl} \times \frac{P_{MT} \times \Delta t}{\eta_{MT}} \quad (1)$$

$$Q_{MT} = \frac{P_{MT} \times \Delta t}{\eta_{MT}} (1 - \eta_{MT} - \eta_l) \quad (2)$$

$$Q_H = Q_{MT} \times \eta_{H.REC} \times \zeta_H \quad (3)$$

$$Q_C = Q_{MT} \times \eta_{C.REC} \times \zeta_C \quad (4)$$

where C_{MT} represents the fuel cost of the MT in the operation time; C_{nl} stands for the natural gas price; P_{MT} is the electricity energy produced by the MT, and η_{MT} represents MT's efficiency; Δt is the dispatch interval time, and it is 1 h in this paper; Q_{MT} is the residual heat of exhaust air after power generation; η_l represents the heat loss factor of the CCHP system; Q_H and Q_C represent the heating and cooling capacity generated from the residual heat of exhaust; $\eta_{H.REC}$ and $\eta_{C.REC}$ are the heat and cooling efficiency, respectively. ζ_H and ζ_C stand for the heating and refrigeration coefficient respectively. For detailed information about PV, WT, FC, DE and ESS, please refer to [43–45].

2.1.2. Improved CCHP Dispatch Strategy

In general, MT is designed to operate in CCHP mode. The electric power generated by MT is only decided by the whole MG's thermal or cooling load. On this occasion, the electric power output of MT is converted from a decision variable to a constant value which is related to the thermal or cooling load only. Consequently, the optimization model for MG is simplified and the effect devoted by MT to operation performance is weakened. Based on the fact that little variation (5% in this paper) in environmental parameters will not have great impacts on people's comfort fell, an improved dispatch strategy for CCHP was presented, as shown in Figure 2 (taking the case of thermal load for example). The basic electric power is determined by MG's thermal load, while the upper limit rises 5% and the

lower limit declines 5% due to the variation margin of indoor environmental parameters. Intuitively, the columns in Figure 2 stand for the adjustable range of an MT’s electric power generation.

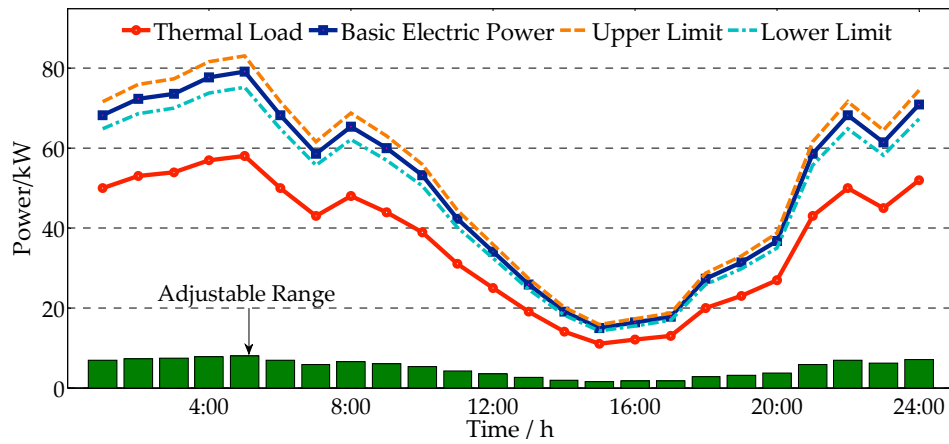


Figure 2. Adjustable range of an MT’s electric power generation.

2.2. Overview of Studied Stand-Alone MG

Figure 3 shows the MG studied in this paper with ESS, FC, PV, WT, MT and DE. Storage battery (SB) is selected as ESS in this paper. In this system, improved dispatch strategy for CCHP was applied. Various types of micro sources and ESS are integrated together in the MG because the operation reliability is the first issue especially for a stand-alone MG which lacks the support from utility grid. As a result, the installation cost is not the most important in some cases such as independent islands or scientific surveys in remote areas. And multi-types of generations could improve the operation stability and reliability. The objective is to get the optimal output combination of DGs and realize optimized operation under the conditions of renewable energy and demand uncertainty. A two-time scale model, consisting of day-ahead scheduling and real-time scheduling, is established for the optimal operation of the stand-alone MG.

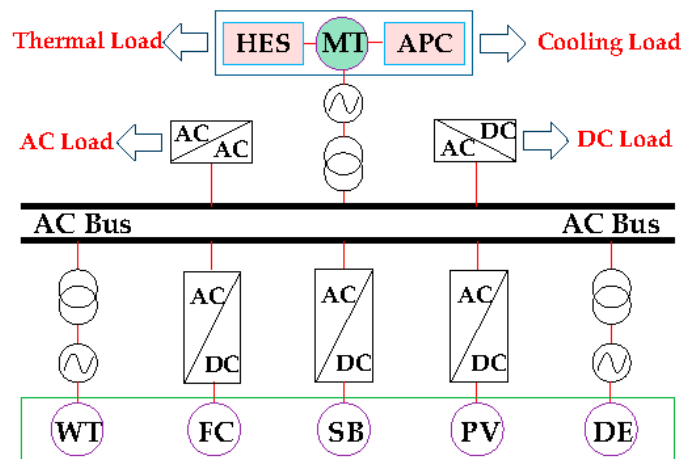


Figure 3. The structure of stand-alone MG.

All the controllable DGs and CLs are dispatched in the day-ahead scheduling on the basis of 24-h forecasted output of WT and PV, while only ESS and CL are dispatched in the real-time because of their fast response speed, and MT or WT was assistant dispatch means at the same time. The overall optimized process is shown in Figure 4.

Day-ahead scheduling provides the rough dispatch scheme while the real-time scheduling makes small adjustments based on the results of day-ahead scheduling to smooth out the actual fluctuations of load and renewable energy relative to predicted data, reducing the disadvantageous impacts. It should be noted that the battery will be charged only in the first time scale.

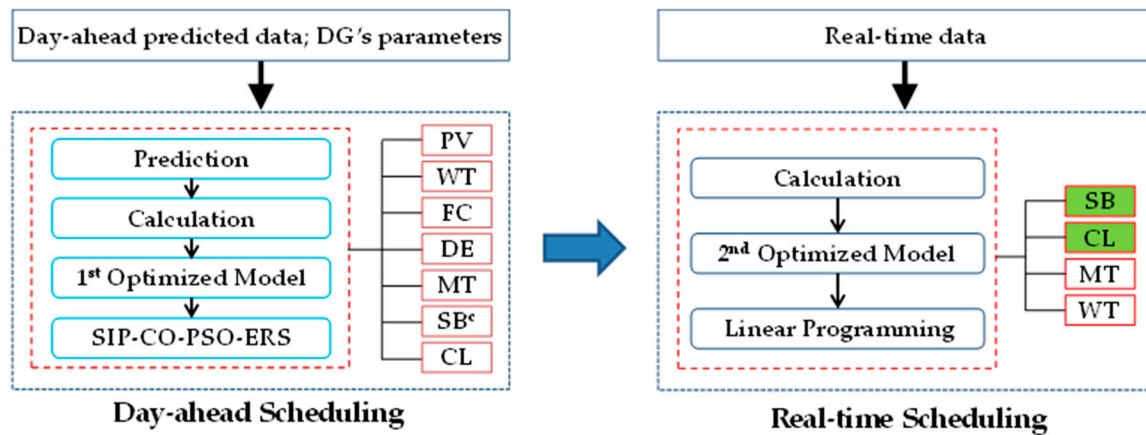


Figure 4. The overall optimized process of two-time scale optimization model.

2.3. The Day-Ahead Scheduling Optimized Model

The first time scale optimization is the day-ahead scheduling, which dispatches the primary outputs of PV, WT, MT, FC, DE, ESS and load control quantity (LCQ) in this paper. For stand-alone MGs, the key operation objective is to keep the power balance within the MG. Consequently, it's better to have more energy supply than load demand rather than less. Considering that the response speed of the battery is fast [46], it will be charged only in this stage, so that in the second time scale, it has enough electricity to discharge rapidly to track the load fluctuation over the predicted data and weaken the influence from predicted errors.

2.3.1. Objective Function in Day-Ahead Scheduling

MG's optimized operation is a multi-objective and multi-constraint minimization optimization problem. This paper adopts the daily 24-h scheduling model in which the load and renewable energy output are supposed to be constant in each dispatch period. The objective function includes three sub-goals which aim to minimize the operation and maintenance cost (OMC) of different DGs, pollutant disposal expense and load control compensation (LCC). The established multi-objective optimization model is:

$$\min F(t) \Rightarrow [F_1(t), F_2(t), F_3(t)] \quad (5)$$

where $F_1(t)$ is the OMC of the whole MG; $F_2(t)$ represents the pollutant disposal cost, and $F_3(t)$ is the LCC of MG. In this paper, all the subgoals are transformed into cost values and the multi-objective model could be converted into a single objective model:

$$\min f(t) = \min [F_1(t) + F_2(t) + F_3(t)] \quad (6)$$

The proposed model is applied to provide a 24-h scheduling scheme of various DGs to minimize the total cost while satisfying the electricity, thermal and cooling load of MG.

(1) Operation and Maintenance Cost (OMC)

The OMCs of micro sources are usually proportional to their power outputs. Supposing that the renewable power generations (WT and PV) have little OMC, then the sub-objective of OMC can be expressed by:

$$F_1(t) = \sum_{i=1}^N (C_i(P_i^t) + K_i P_i^t \Delta t) + K_H P_H^t \Delta t + K_C P_C^t \Delta t \quad (7)$$

where P_i^t and $C_i(P_i^t)$ are the generation output and fuel cost of micro source i in the t -th dispatch period. K_i , K_H , K_C are the maintenance factor of micro source i , HES and AC modules. P_H^t and P_C^t represent the heat power generated by HES and the cooling power generated by AC, respectively.

(2) Pollutant Disposal Cost

MT, DE and FC would release NO_X , CO_2 , SO_2 and other pollutants into air during generation. And the emission coefficients of pollutant disposal are different for diverse generation units and different impacts on the environment as well [47]. In this paper, the pollutant disposal cost was considered by Equation (8):

$$F_2(t) = \sum_{i=1}^N \sum_{k=1}^M \alpha_k \times E_{ik} \times P_i^t \times \Delta t \quad (8)$$

where E_{ik} is the released quantity of pollutant k when micro source i lets out unit power; N is the number of generation units while M is the number of pollutant types. α_k is the conversion coefficient for various pollutant (NO_X , CO_2 , SO_2).

(3) Load Control Compensation (LCC)

To take the advantage of demand side management and improve the operation reliability, CL was considered, which could also act as an auxiliary resource to MG's power balance. The LCC is corresponding to the reliability cost of the MG. It's difficult to calculate the reliability cost strictly in theory. Generally, it's given by the product of expected energy not supplied (EENS) and unit interruption cost (UIC). In this paper, the EENS was representative by LCQ which took the whole MG's operation economy and reliability into account, and the corresponding compensatory costs were calculated as follows:

$$F_3(t) = p_D^t \times P_{cut}^t \quad (9)$$

where p_D^t is the UIC of MG and P_{cut}^t is the LCQ.

2.3.2. Operation Constraints in Day-Ahead Scheduling

In terms of MG's optimized operation, constraints like security, reliability and power balance must be guaranteed [48]. These constraints can be divided into equality constraints and inequality constraints.

(1) Power Balance Constraint:

$$\sum_{i=1}^K P_i = P_L - P_{cut} \quad (10)$$

$$Q_H = Q_{HL} \quad (11)$$

$$Q_C = Q_{CL} \quad (12)$$

where P_i is the output of generation unit i ; P_L and P_{cut} are the load demand and load control power, respectively. Q_{HL} and Q_{CL} represent the thermal and cooling load independently; Q_H and Q_C are the thermal and cooling power supplied by micro sources.

(2) Output Constraint:

$$P_{imin} \leq P_i^t \leq P_{imax} \quad (13)$$

where P_{imin} and P_{imax} are the minimum and maximum power output of generation unit i .

(3) Ramp Up/Down Rate Constraint:

$$P_i^t - P_i^{t-1} \leq R_{up}\Delta t \quad (14)$$

$$P_i^{t-1} - P_i^t \leq R_{down}\Delta t \quad (15)$$

where R_{up} and R_{down} are the ramp up/down rate of micro source i . P_i^t and P_i^{t-1} represent the output of micro source i in the current and last dispatch interval.

(4) Battery Operation Constraint:

$$S_{SOC.min} < S_{SOC} < S_{SOC.max} \quad (16)$$

$$-K_C Q_B \eta_{SBC} \leq P_{SB}^t \leq K_D Q_B \eta_{SBD} \quad (17)$$

where $S_{SOC.min}$ and $S_{SOC.max}$ are the minimum and maximum state of charge (SOC) for the battery. K_C and K_D are the maximum charging/discharging proportion in a dispatch interval, while P_{SB}^t is the battery's power output in the t -th period. η_{SBC} and η_{SBD} represent the charge/discharge efficiency. Q_B represents the capacity of battery.

(5) Load Control Constraint:

$$P_{cut}^t \leq P_{cut.max} \quad (18)$$

where P_{cut}^t is the LCQ in the t -th dispatch interval and $P_{cut.max}$ is the load control upper limit of MG.

(6) MT's Electric Output Constraint:

$$0.95P_{E,MT} \leq P_{E,MT} \leq 1.05P_{E,MT} \quad (19)$$

where $P_{E,MT}$ is the electric output of MT.

2.4. The Real-Time Scheduling Optimized Model

The second time scale optimization is the real-time scheduling which further adjusts the battery discharge and load control to realize the power balance in real time. The coordinated operation of ESS and CL is put forward to reduce the impact of renewable energy and demand uncertainty, making the best of their fast response characteristic. A unified prediction error percentage (UPEP) is defined to describe the difference between the actual and predicted load demand:

$$\Delta E\% = \frac{(\Delta P_E - \Delta P_{PV} - \Delta P_{WT} - \Delta P_{MT})}{P_{Re}} \times 100\% \quad (20)$$

$$\Delta H\% = \frac{\Delta H}{H_{Re}} \times 100\% \quad (21)$$

$$\Delta C\% = \frac{\Delta C}{C_{Re}} \times 100\% \quad (22)$$

where $\Delta E\%$, $\Delta H\%$ and $\Delta C\%$ are the UPEP of electric, heat and cooling load demands, respectively. P_{Re} , H_{Re} and C_{Re} represent the predicted electric, heat and cooling load demands. ΔP_E , ΔH and ΔC are the differences of actual and predicted electric, heat and cooling load demands. ΔP_{PV} , ΔP_{WT} and ΔP_{MT} stand for the differences between actual and predicted electric outputs of PV, WT and MT, respectively. $\Delta E\%$, $\Delta H\%$ and $\Delta C\%$ are the error quantization of predicted data.

2.4.1. Objective Function in Real-Time Scheduling

In this stage, the decision variables have decreased and the model has become simpler. The dispatch objects are mainly CL and battery, which can respond rapidly to eliminate the errors in the last scheduling and realize optimal economy, while WT and MT remain auxiliary means. The objectives consist of OMC and LCC; the model can also be converted into single-objective optimization.

(1) OMC Adjustment in Real-time Operation:

$$F_4(t) = (K_{ES}P_{ES}^t + K_{MT}\Delta P_{MT}^t + K_H\Delta P_H^t + K_C\Delta P_C^t + C_{MT}(\Delta P_{MT}^t)) \times \Delta t \quad (23)$$

where K_{ES} and K_{MT} are the maintenance factors of ESS and MT. P_{ES}^t is the charge/discharge quantity of ESS. ΔP_{MT}^t , ΔP_H^t and ΔP_C^t are the output adjustments of MT between two time scales, predicted error of heat and cooling load demand, respectively. $C_{MT}(\Delta P_{MT}^t)$ stands for the change of fuel cost change for MT.

(2) LCC Adjustment in Real-time Operation:

$$F_5(t) = p_D^t \times \Delta P_{cut}^t \quad (24)$$

where ΔP_{cut}^t is the LCQ differences between two time scales.

2.4.2. Operation Constraints in Real-Time Scheduling

In this time scale, constraints (1), (4), (5) and (6) in the day-ahead scheduling model will be satisfied.

3. SIP-CO-PSO-ERS Algorithm

For a multi-objective optimization problem, the best condition is to find the absolute optimal solution. However, subgoals are usually contradictory with each other and it's impossible to find a common solution that makes all the sub-goals achieve optimal values at the same time. Therefore, the multi-objective model is transformed into a weighted single-objective model to optimize the whole system's operation cost. Considering that the model of the first time scale has been converted into single-objective optimization model, this paper proposes SIP-CO-PSO-ERS to solve the day-ahead scheduling model. Fewer decision variables and constraints simplify the model in the second time scale. Linear programming in MATLAB/Optimization Tool (R2011B, MathWorks, Natick, MA, USA) was conducted to solve the real-time scheduling model.

3.1. Basic PSO Algorithm

PSO is a meta-heuristic intelligent algorithm on the basis of population search [49]. The individuals of population update their velocity vectors according to their own speed, individual optimal solution p_{best} and population optimal solution g_{best} to converge to global optimal solution during all the iterations. The velocity and position for particle i at moment t are updated as follows:

$$v_{i,j}(t+1) = wv_{i,j}(t) + c_1r_1(p_{i,j} - x_{i,j}(t)) + c_2r_2(p_{g,j} - x_{i,j}(t)) \quad (25)$$

$$x_{i,j}(t+1) = x_{i,j}(t) + v_{i,j}(t+1), j = 1, 2, \dots, d \quad (26)$$

where w is the inertia weight for PSO; c_1 and c_2 are both learning factors; r_1 and r_2 are random numbers between 0 and 1; d is the dimension of the optimization problem; $p_{i,j}$ and $p_{g,j}$ represent the individual and population optimal solution. $v_{i,j}(t)$ and $v_{i,j}(t+1)$ are the velocity vectors for particle i in the j -th dimension at moment t and $t+1$; accordingly, $x_{i,j}(t)$ and $x_{i,j}(t+1)$ are the position vectors for particle i in the j -th dimension at moment t and $t+1$.

Due to the full use of individuals' and group's experience, the PSO algorithm is able to approach the optimal solution with a relatively high convergence efficiency [50]. Because of the consideration of CL and multi-scenarios, more decision variables, constraints, and intricate data for variable scenarios complicate the optimization model. Therefore, the PSO exhibits the problems of premature, poor local and global search ability when solving the optimized operation model of stand-alone MG [51]. Specially, a fall into the local optimum because of the oscillation around certain local optimums with inappropriate step lengths would occur. In addition, the convergence speed is slow in later iterations because the optimum search goes beyond the constraints easily when there is great fluctuation in predicted data from different scenarios, causing the process to repeat several times until the constraints are all satisfied. However, the MG's day-ahead optimized scheduling requires not only a faster solution speed to meet the dispatch timeliness, but also an excellent search performance to satisfy dispatch accuracy. Reasonable modification must be developed to improve the properties of basic PSO. In this paper, a dual-step modification consisting of SIP and CO is introduced into PSO as well as ERS.

3.2. Search Improvement Process (SIP)

Considering that a local optimum cannot take full advantages of different DGs for a stand-alone MG in economy and environmental protection, the total ability of PSO in both global and local optimizing must be improved. SIP was conducted on all the particles during the optimization to improve the global search ability for PSO. The global search ability improvement of proposed SIP is based on [52]:

- (1) Increasing the population's diversity by mutations and cross operations.
- (2) Promoting all the particles to move toward the best promising local or global individuals.

After the update of both velocity and position vectors for particle i , a modified process was carried out as follows:

- (1) Find out the best individual X_{best} and the worst individual X_{worst} through the calculation of fitness function.
- (2) For each particle i , two particles X_m and X_n are selected from the particle swarm randomly such that $m \neq n \neq i$, then the following two particles are generated by cross style:

$$X_{cross}^1 = X_i + \Delta \times (X_m - X_n) \quad (27)$$

$$X_{cross}^2 = X_{cross}^1 + \Delta \times (X_{best} - X_{worst}) \quad (28)$$

where Δ is a random number between 0 and 1, X_{cross}^1 and X_{cross}^2 are two new particles obtained by cross.

- (3) A mutation process is implemented after the cross to get five new particles, and the j -th dimensions of X_{muta}^1 , X_{muta}^2 , X_{muta}^3 , X_{muta}^4 and X_{muta}^5 are obtained by:

$$X_{muta,j}^1 = \lambda_1 \times X_{best} + \lambda_2 \times X_{worst} \quad (29)$$

$$X_{muta,j}^2 = \begin{cases} X_{best,j} & \text{if } k_1 \geq k_2 \\ X_{i,j} & \text{if } k_1 < k_2 \end{cases} \quad (30)$$

$$X_{muta,j}^3 = \begin{cases} X_{best,j} & \text{if } k_3 \geq k_4 \\ X_{cross,j}^1 & \text{if } k_3 < k_4 \end{cases} \quad (31)$$

$$X_{muta,j}^4 = \begin{cases} X_{best,j} & \text{if } k_5 \geq k_6 \\ X_{cross,j}^2 & \text{if } k_5 < k_6 \end{cases} \quad (32)$$

$$X_{muta,j}^5 = \begin{cases} X_{cross,j}^1 & \text{if } k_7 \geq k_8 \\ X_{cross,j}^2 & \text{if } k_7 < k_8 \end{cases} \quad (33)$$

where $k_1, k_2, \dots, k_8, \lambda_1$ and λ_2 are all random numbers range from 0 to 1; Equation $\lambda_1 + \lambda_2 = 1$ is satisfied.

- (4) Then the best particle among $X_{muta}^1, X_{muta}^2, X_{muta}^3, X_{muta}^4$ and X_{muta}^5 is selected by fitness values to compare with X_i . If it is better than X_i , replace X_i with the selected particle; otherwise, X_i will remain in the initial position. After SIP, CO will be conducted.

3.3. Chaotic Optimization (CO)

The ergodicity and randomness characteristics of chaos could realize local deep search [53]. Better local optimized ability is achieved by searching the space near superior individuals. The basic principle for chaotic optimization-particle swarm optimization (CO-PSO) to strength the local search ability is mapping the chaotic variables into the optimized variables' space linearly. For a given optimization target, the search process is corresponding to the traversal process of chaotic orbit. The steps of chaotic search in this paper are indicated as:

- (1) Suppose $k = 0$, and map the decision variables $x_j^k, j = 1, 2 \dots d$ into chaotic variables s_j^k between 0~1 for every dimension of the solution. $x_{max,j}$ and $x_{min,j}$ are the upper and lower search bounds of the j -th dimension:

$$s_j^k = \frac{x_j^k - x_{min,j}}{x_{max,j} - x_{min,j}}, j = 1, 2 \dots d \quad (34)$$

- (2) Calculate the chaotic variables of the next iteration:

$$s_j^{k+1} = 4 \times s_j^k (1 - s_j^k), j = 1, 2 \dots d \quad (35)$$

- (3) Convert the chaotic variables s_j^{k+1} into decision variable x_j^{k+1} by the following formula:

$$x_j^{k+1} = x_{min,j} + s_j^{k+1} (x_{max,j} - x_{min,j}), j = 1, 2 \dots d \quad (36)$$

- (4) Assess the new obtained solution by x_j^{k+1} . Make a decision by different result: if the new obtained solution is better than the initial one or the chaotic search has reached the maximum iteration, the new obtained solution will be the final result of chaotic search; otherwise, set $k = k + 1$ and turn to Step 2.

In this paper, the first 20% of the best particles during each iteration are chaotic searched in order to further excavate the adaptability of excellent particles and improve the local search ability of optimization algorithm.

3.4. Elite Retention Strategy (ERS)

The premature of an optimization algorithm is caused by the loss of population diversity, which is due to the population's pattern simplification in later iteration. It is an obstacle to find the global optimal solution during the stand-alone MG's optimized operation. ERS is a procedure to preserve the optimal individuals, or a part of excellent individuals during each iteration, and replace the worst individuals at the beginning of next iteration. The ERS could avoid the loss of better solutions generated during each iteration and maximize the advantages of superior individuals. That is to say, poor solutions will be superseded as soon as possible. In addition, the population diversity is guaranteed because of the reservation of initial particles at the beginning of each iteration as well as the connection between two generations. Through this process, the premature phenomena will be impaired and the convergence speed is accelerated. In this paper, ERS is integrated into basic PSO algorithm.

Specifically, the top 10% of the best individuals are reserved at the beginning of each iteration. Then the last 10% of the population in next-generation individuals will be replaced correspondingly.

3.5. Detailed Procedures of SIP-CO-PSO-ERS

Figure 5 exhibits the structure of presented algorithm and the detailed procedures of SIP-CO-PSO-ERS in this paper are given as follows:

- (1) Initialize the position and velocity of each particle in the population.
- (2) Assess the fitness of each particle by objective function calculation.
- (3) Preserve current particles' positions and fitness values into p_{best} of each particle; preserve the position and fitness value of the optimal individual in current population into g_{best} .
- (4) Save the top 10% of the best individuals whose fitness values are the best.
- (5) Execute the SIP on all particles.
- (6) Evaluate the fitness of each particle and search the top 20% of best individuals with CO; update p_{best} and g_{best} of the whole population.
- (7) If the solution has reached the required search accuracy or the maximum iteration, stop the chaotic search and export the result, otherwise, turn to step 8.
- (8) Update the position and speed of each particle; evaluate all particles' fitness values and replace the last 10% individuals with the worst fitness by the best individuals preserved in step 4, then turn to step 3.

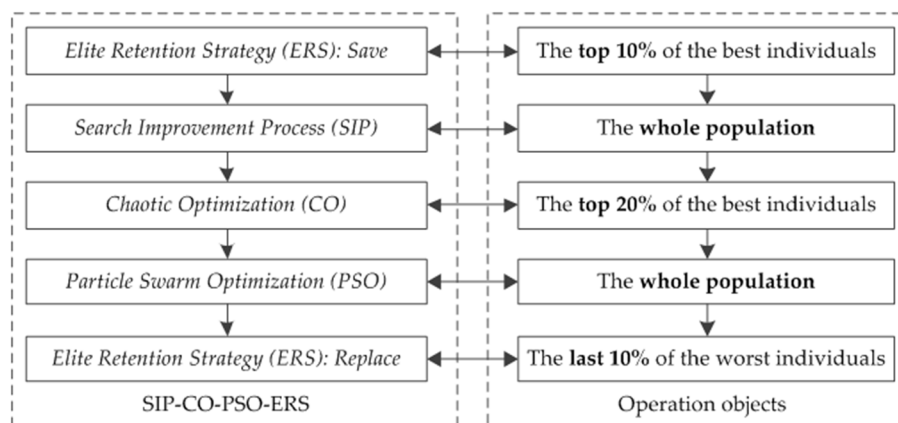


Figure 5. Structure of the proposed SIP-CO-PSO-ERS.

3.6. The Limitations of Proposed SIP-CO-PSO-ERS

SIP-CO-PSO-ERS has many advantages such as better adaptability, fast convergence speed and excellent search ability. However, limitations are also existed, as follows:

- (1) SIP-CO-PSO-ERS consists of different procedure modules due to the algorithm integration. As a result, it's really hard work for programmers to write the program correctly. Any errors in the code would lead to a wrong operational result. More time should be spent on the programming so as to ensure the correct code;
- (2) The particles that are generated randomly increase the operation time to some extent. When the proposed model and SIP-CO-PSO-ERS are applied in a specific MG, initial values of particles could be given according to MG's historical operation states so as to decrease the iteration numbers and operation time.

3.7. The Framework of Stand-Alone MG's Optimized Operation

Figure 6 shows the integrated framework of this study about the optimized operation for proposed stand-alone MG in detail. The final dispatch scheme is obtained by the results of day-ahead and real-time scheduling models.

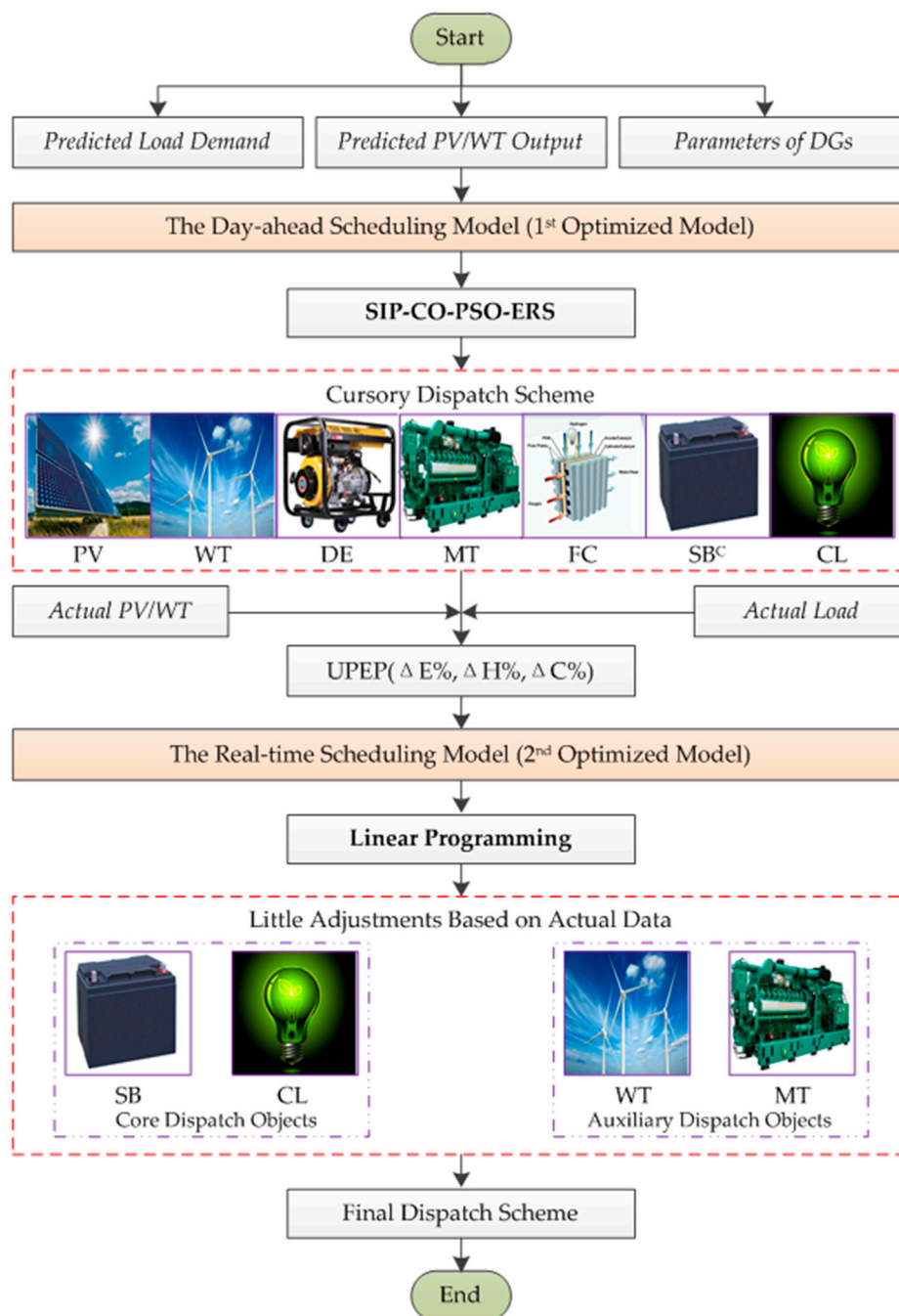


Figure 6. Integrated framework of the whole study.

4. Simulation Analysis

4.1. Description of the Stand-Alone MG system

The stand-alone MG adopted in this paper is shown in Figure 3. The battery's parameters are as follows [54]: the self-discharge rate is 0.14%, charge/discharge efficiency is 92%, minimum SOC

is 20%, total capacity is 50 kWh while the lower limit is assuming as the initial SOC. The efficiency of convertors is assumed to be 95%. Rated power of PV and WT is assumed to be 250 kW and 300 kW, respectively. The proportion of CL is assumed as 10%. Other parameters of different DGs are summarized in Table 1. Table 2 lists the disposal cost for different kinds of pollutants and the respective pollutant emission factors of MT, DE and FC [55,56]. The simulation in this paper takes winter for example, so thermal load (TL) is included except electric load (EL).

Table 1. Parameters setting of various DGs.

Type	P_e (kW)	P_{max}/P_{min} (kW)	R_{up}/R_{down} (kW/min)	K (\$/kWh)
DE	150	180/10	20	0.01258
FC	130	160/10	10	0.00419
MT	100	125/10	10	0.00587
ESS	25	-	-	0.01241

Table 2. Pollutant disposal cost and emission factors.

Type	Disposal Cost (\$/lb)	DE(lb/kWh)	FC (lb/kWh)	MT (lb/kWh)
NO_x	4.2	2.18×10^{-2}	3×10^{-5}	4.4×10^{-4}
SO_2	0.99	4.54×10^{-4}	6×10^{-6}	8×10^{-6}
CO_2	0.014	1.432×10^{-3}	1.078×10^{-3}	1.596×10^{-3}

4.2. Results Analysis

In order to analyze and compare the optimized dispatch problem in various situations and verify the proposed model, different scenarios are designed in this paper for the stand-alone MG. Since the load demand in work day differs from that in weekend, and the output of PVs in sunny day differs greatly from that in rainy day, four scenarios are chosen for the designed stand-alone MG: sunny-work day, sunny-weekend, rainy-work day and rainy-weekend scenario. The predicted load demand and renewable power generation in different scenarios are displayed in Figure 7.

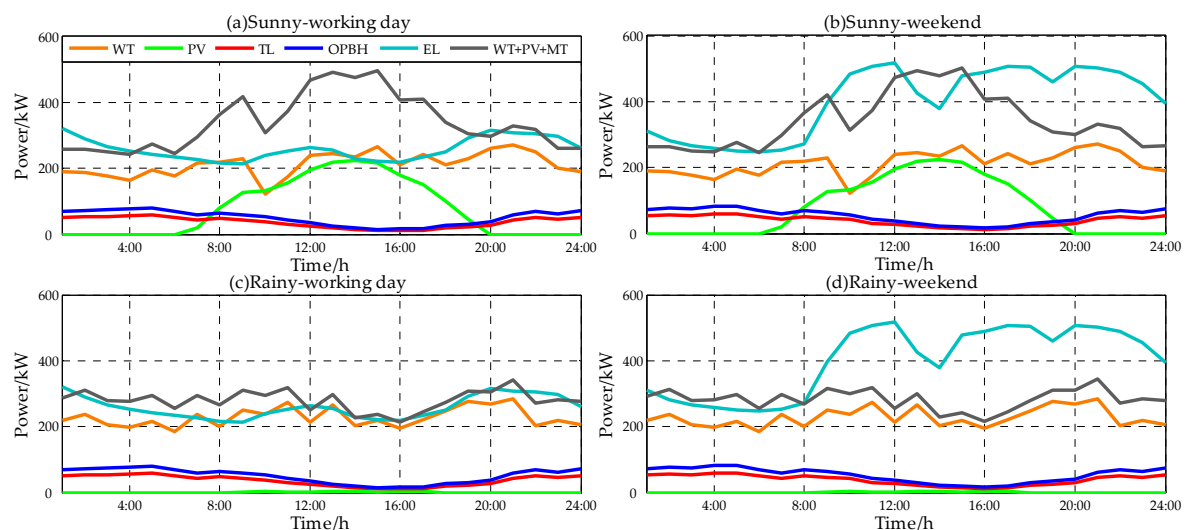


Figure 7. The load demand and predicted renewable power generations in four scenarios for MG.

Figure 7 shows clearly that the output of renewable generations in sunny days and rainy days is quite different: the overall output of renewable energy in sunny days is larger, and peak time intervals are concentrated in 11:00~15:00. Because of the weakness of solar radiation in rainy days, the PV's power output is very low. As a result, the main output of renewable energy is wind power under these conditions. The load change is closely related to the activities of people. Based on the fact that the

main load type in a stand-alone MG is from residents, the EL demand of weekends is obviously higher than that of work days, while the thermal load demand performs a relatively little fluctuation between work days and weekends.

4.2.1. The Day-Ahead Scheduling Results

SIP-CO-PSO-ERS was used to solve the day-ahead scheduling model. For the algorithm, the iteration numbers of CO and PSO are set as 10 and 200 respectively. The particles' number is 30, inertia weight is 0.5, and the learning factors are both 2. PV modules are under the control of a maximum power point tracking (MPPT) strategy. When the total electric output of PV, WT and MT (ordering power by heat, OPBH) is higher than the load demand, and the battery has reached the upper limit of capacity, WT is adjusted to track the load demand. Otherwise the WT modules are also under the control of MPPT. Figure 8 shows the optimized results of the first time scale in different scenarios.

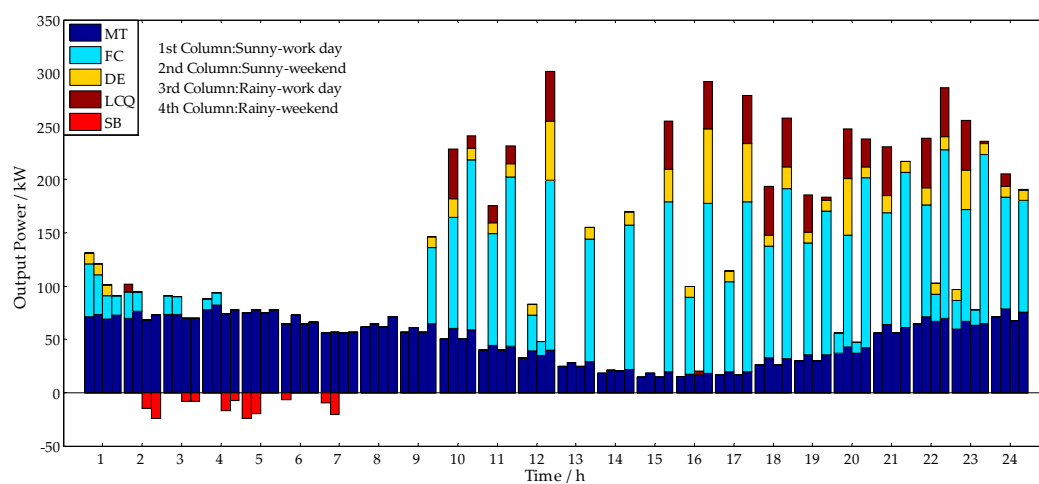


Figure 8. The optimized results in each period for four scenarios in the first time scale.

The model takes consideration of load control in a stand-alone MG. The simulation results in Figure 8 show that the load control which is corresponding to LCQ column of the figure is inconspicuous in sunny-work day and rainy-work day scenarios because of the low demand and sufficient energy supply. In contrast, load control effect is apparent in sunny-weekend and rainy-weekend scenarios and concentrated in two periods (noon and night) of a day. Compared with Figure 7, it's obvious that the load control mainly takes place in the periods with inadequate renewable outputs relative to the load demand. For a stand-alone MG, other DGs like DE, MT and FC must be started to maintain the power balance if the renewable energy is insufficient. When the LCC is lower than the generation cost of DGs, the system will cut off part of unimportant load to maximize the operational economy. In addition, load control is more common in rainy-weekend scenario than sunny-weekend scenario, because the low PV output in rainy-weekend scenario further expands the difference between renewable energy output and load demand. In case of emergency, load control is not only a measure to improve the system economy, but also an auxiliary resource to maintain stability and power balance for stand-alone MG.

The SOC variation of battery is related to whether the sum of renewable energy and basic output (decided by thermal load demand) of MT is higher than EL demand. If the condition is satisfied, the battery will be charged. For instance, in rainy-weekend scenario, the EL demand is relatively high and PV output is low, which results in the EL demand being higher than the sum of renewable energy and MT's basic output after 8:00; accordingly, there is no redundant electric power for the battery to charge in these periods. And the SOC of battery will decrease slowly because of the self-discharge

effect. However, before 8:00, the conditions are opposite and the battery is charged. If the battery is being charged, it indicates that the power of the whole system is surplus. Therefore, the outputs of DE and FC are 0, which is consistent with the actual situation.

Figure 8 also indicates that the FC was preferential dispatched than DE within a certain range, because the model considers the economic and environmental benefits. And FC is more eco-friendly than DE according to Table 2. Based on the optimized model, 24-h'operation costs of four scenarios for each day in the first time scale scheduling are shown in Figure 9.

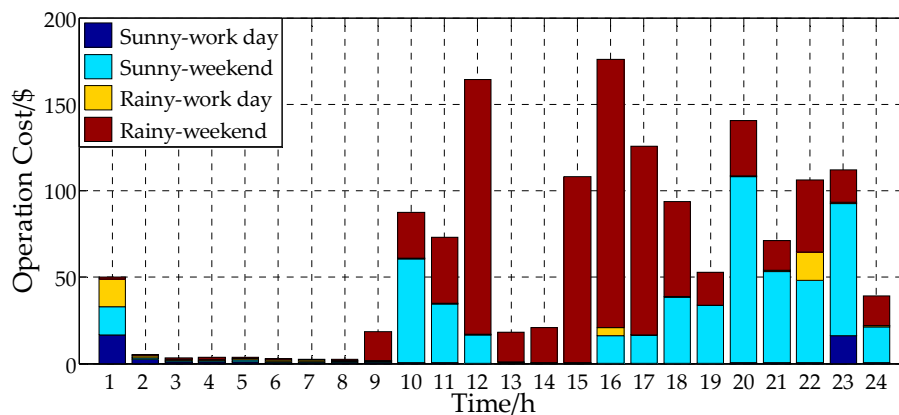


Figure 9. Total operation costs of four scenarios in the first time scale.

If the sum of renewable energy and MT's basic output is higher or close to EL demand, the total operation cost will be low. For example, in sunny-work day, the sum output of WT, PV and MT is higher than EL demand from 7:00 to 18:00; accordingly, the operation costs in these periods are very low. Only WT, PV and MT are running in the whole system when battery's SOC reaches the upper limit. The MG tracks the EL change by adjusting WT's output. When the EL demand is greater than the sum of renewable energy and MT's basic output, the cost increases due to the expenses generated by other DGs. Comparing the four scenarios, it could be found that the costs of sunny-weekend and rainy-weekend are signally higher than that of work day scenarios. That's due to the higher load demand on weekend scenarios. On the other hand, the cost of rainy-weekend is higher than that of sunny-weekend because of the lower PV output during rainy days.

This paper proposes an improved dispatch strategy for CCHP operation mode under the condition where the essential load demand is not influenced. The electric output of MT is variable from 95~105% of the basic electric demand ordered by the thermal load. To verify the effectiveness of the improved strategy, simulation with the same conditions except CCHP's strategy of four scenarios was carried out. Table 3 shows the results of operation costs.

Table 3. Comparison of CCHP's improved and general strategy.

Scenario	Sunny-Workday	Sunny-Weekend	Rainy-Work Day	Rainy-Weekend
Improved Strategy (\$)	45.694	543.358	48.067	845.266
Traditional Strategy (\$)	47.207	581.512	50.153	901.072
Cost Decrease (%)	3.21	6.56	4.16	6.19
Load Demand (kW)	1201.761	1268.601	1201.761	1268.601
Actual Output (kW)	1164.591	1280.596	1160.254	1263.831
Demand Deviation (%)	3.09	-0.95	3.45	0.38

From the table, it is evident that the MG's economic and environmental benefits are improved in all the scenarios without destroying the comfort feel and primary demand. For example, in rainy-weekend scenario, the total operation cost decreased 6.19% at the expense of 0.38% load variation. And the improved CCHP strategy was obviously more effective in weekend scenarios, because the adjustment

margin of iterative optimization was more extensive as a result of higher electric demand during the weekend.

4.2.2. The Real-Time Scheduling Results

The real-time scheduling model mainly dispatches the CL and ESS to overcome the errors between actual data and predicted data for load demand and renewable energy. The error of EL demand and renewable energy is uniformly expressed by the UPEP, which represents the total electricity variation. Fluctuations of EL and thermal load are simulated by Monte-Carlo simulation and the model is solved by linear programming in the MATLAB Optimization Tool. Table 4 exhibits the simulation results of $\Delta E\%$ and $\Delta H\%$ by Monte-Carlo simulation, while Figure 10 shows the optimized results in four scenarios including the adjustment quantity (AQ) of the battery, the CL, and the cost variation.

Table 4. Comparison of improved and traditional strategy for CCHP.

Interval	Sunny-Work Day		Sunny-Weekend		Rainy-Work Day		Rainy-Weekend	
	$\Delta E\%$	$\Delta H\%$	$\Delta E\%$	$\Delta H\%$	$\Delta E\%$	$\Delta H\%$	$\Delta E\%$	$\Delta H\%$
1, 2, 3	-1, 2, -5	-3, 2, 2	2, 2, 3	-2, 2, 1	5, 4, -1	-3, 1, 3	3, -2, -2	-2, 3, 3
4, 5, 6	5, -1, 3	2, 2, 3	-4, 5, -1	-3, -2, -3	-5, 1, 4	-2, 3, -1	5, -1, -3	-3, 1, 3
7, 8, 9	-5, -3, -4	2, 3, 3	-3, -1, -1	2, -1, 2	4, 2, 4	-2, 3, -2	4, 2, -5	1, -2, 1
10, 11, 12	-5, -3, 3	-2, -3, 2	4, -2, 3	1, 1, -1	-5, 3, 5	-2, 2, 2	4, 5, 1	-3, 2, -2
13, 14, 15	-3, -2, -1	-3, 3, 2	5, -3, 2	3, -1, 3	3, 5, 3	-2, -2, -2	-4, 5, -5	1, -2, 3
16, 17, 18	-2, 3, -5	-1, 1, -2	2, 4, -5	-3, -3, 2	5, -3, 1	-1, -1, -3	1, 1, -5	2, -2, -1
19, 20, 21	-4, 3, 5	2, -1, 3	-4, -1, -4	2, 2, 1	1, -2, 1	2, 2, -1	-5, 2, 4	3, 1, 1
22, 23, 24	5, 5, -1	-2, 2, 3	3, -1, -3	1, -1, -3	-5, -2, 3	1, -2, 1	-3, 3, 4	-1, 2, -2

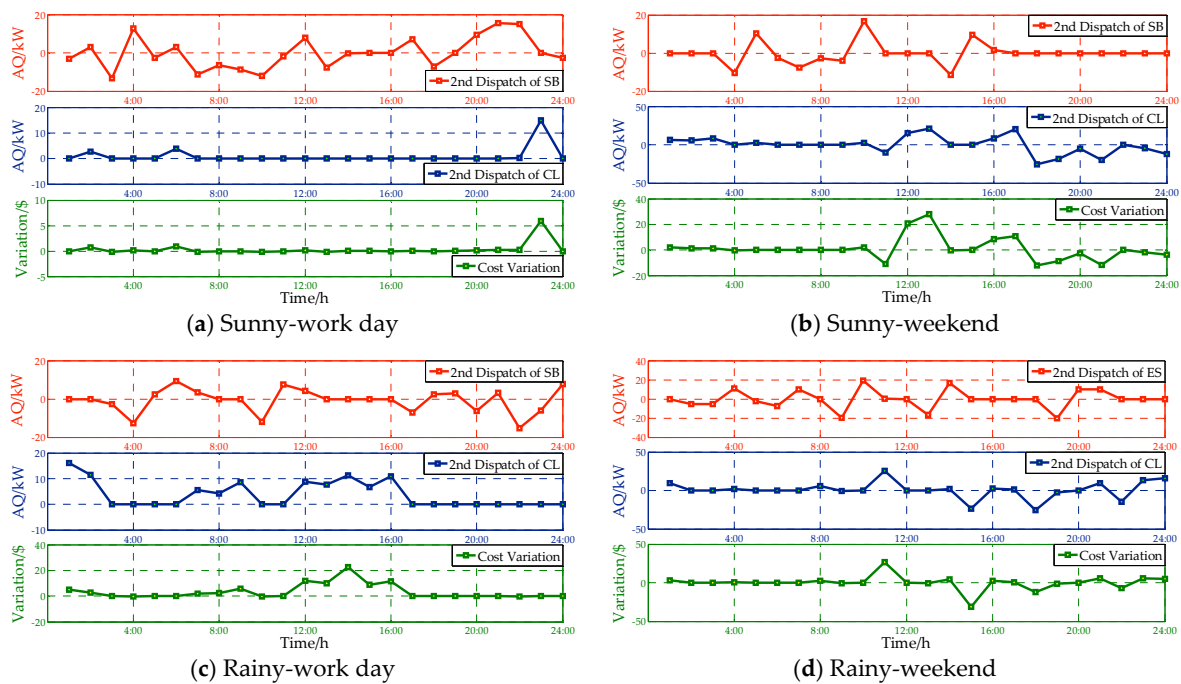


Figure 10. The scheduling results of four different scenarios in the second time scale.

Based on the results in the first time scale, Figure 10 reveals the minor adjustments of battery and CL, which aims to track the actual demand variation. Positive values of the battery represents discharge state while negative values stand for charge state. The positive adjustment of CL corresponds to a LCQ increase while the negative adjustment represents LCQ decrease. It can be seen that the cost variation primarily depends on the CL adjustment because the cost of battery is low. The battery is dispatched first when the actual demand is higher than predicted demand due to the economy. On the other hand, CL is adjusted prior than the battery when the predicted demand is higher than

actual demand. For instance, during the 14th period of rainy-weekend scenario, the $\Delta E\%$ was 5% and the $\Delta H\%$ was -2% . According to the optimized objective, the battery discharged 16.732 kW first and then the CL cut 2.157 kW, because the battery had reached the lower limit of capacity. In the 9th period of sunny-work day scenario, the $\Delta E\%$ was -4% and the $\Delta H\%$ was 3%. Noticing that the LCQ of this period in the first time scale was 0, so the battery was charged instead of the LCQ decreased. Otherwise, LCQ would decrease first and if it was reduced to 0, the battery would charge.

4.2.3. Algorithm Evaluation

To compare the effectiveness of different optimization algorithms, PSO, CO-PSO and SIP-CO-PSO-ERS are used to solve the same model under rainy-weekend scenario in the first time scale. The averaged costs and convergence time for 20 trials are given in Table 5.

Table 5. Statistics of 20 operating results for three different optimization algorithms.

Algorithms	Total Cost		Average Convergence Time/s
	Average Value/\$	Standard Deviation /\$	
PSO	859.677	1.984	176.49
CO-PSO	852.142	1.501	142.91
SIP-CO-PSO-ERS	845.373	0.361	104.43

According to Table 5, it can be found that SIP-CO-PSO-ERS provided the lowest average total operation cost over the 20 trials, which reveals a better searching and convergence performance. This is because ERS combined with the dual-step modification was able to excavate the best individuals, improving the global and local search ability for optimization algorithm. The lowest standard deviation of the SIP-CO-PSO-ERS indicates that the algorithm was stable and strongly robust. The SIP-CO-PSO-ERS also had some superiority on convergence speed due to the adoption of ERS.

Figure 11 shows the iterative process of three algorithms in the first period of sunny-work day scenario. From the figure, values of the objective function of all the algorithms decrease gradually along the iteration, which indicates that the algorithms searched in a favorable direction and finally reached a stable value. However, the SIP-CO-PSO-ERS can converge to a better solution much faster because of the introduction of dual-step modification and the ERS, which made full use of the “survival of the fittest” principle under the premise of population diversity.

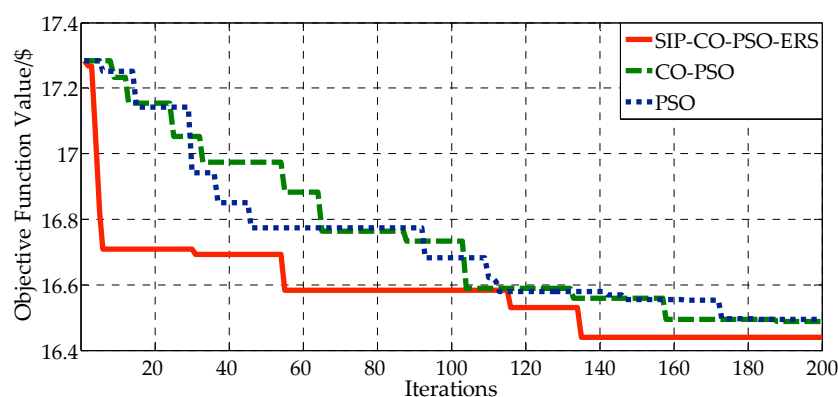


Figure 11. Iterative process comparison of three algorithms.

5. Conclusions

In this paper, a comprehensive optimized operation model is presented for a stand-alone MG. It's of great significance to keep the power balance and decrease the operation cost especially for stand-alone MG. The MG was composed of PV, WT, MT, DE, FC and ESS with the consideration of

CL. A two-time scale multi-objective optimization model was developed based on MT's CCHP mode. The dual-step modification and ERS were combined into the PSO to strengthen the global and local search ability as well as improve the convergence speed. An enhanced dispatch strategy for CCHP and the proposed SIP-CO-PSO-ERS algorithm were applied to solve the model in the first time scale with related constraints. The presented SIP-CO-PSO-ERS effectively deal with the stand-alone MG's optimized operation of different scenarios and the improved CCHP strategy significantly enhances the economic and environmental benefits. SIP-CO-PSO-ERS improved the operation economy with about 1.66% average cost decrease and robustness with better standard deviation than general algorithms. In addition, the average convergence time has also decreased about 40.83% compared with PSO which is common used in MG's optimization solution. In other words, it will promote the application of renewable energies in some degree. The coordinated operation of ESS and CL reduced the impact of renewable energy and demand uncertainty effectively in real-time scheduling. After the optimized dispatch, the MG achieves economic operation while the load demands are satisfied. For this paper, the data observation for one day is 24. More detailed time density will be considered in the future to improve the real-time dispatch precision. And effective DR control and coordination schemes which could deal with the simultaneous existence of multiple DR techniques in the same MG are required to be contained in the optimization model in the future.

Acknowledgments: This work was supported in part by the National Natural Science Foundation of China (grant No. 51577067), the Beijing Natural Science Foundation of China (grant No. 3162033), the Hebei Natural Science Foundation of China (grant No. E2015502060), the State Key Laboratory of Alternate Electrical Power System with Renewable Energy Sources (grant Nos. LAPS16007, LAPS16015), the Science & Technology Project of State Grid Corporation of China (SGCC), the Open Fund of State Key Laboratory of Operation and Control of Renewable Energy & Storage Systems (China Electric Power Research Institute) (No. 5242001600FB), the China Scholarship Council. The authors would like to acknowledge Fangxing Li with The University of Tennessee, Knoxville, USA, Saber Talari with University of Beira Interior, Portugal, for their contributions and suggestions to this manuscript.

Author Contributions: All authors have worked on this manuscript together, and all authors have read and approved the final manuscript.

Conflicts of Interest: The authors declare no conflict of interest.

Nomenclature

DGs	Distributed generations	MGs	Microgrids
MTs	Micro-gas turbines	DEs	Diesel engines
FCs	Fuel cells	PVs	Photovoltaics
WTs	Wind turbines	DR	Demand response
ESS	Energy storage system	CL	Controllable load
PSO	Particle swarm optimization	CO	Chaotic optimization
ERS	Elite retention strategy	SIP	Search improvement process
APC	Absorption chiller	HES	Heat-exchanging system
C_{MT}	The fuel cost of MT	C_{nl}	The natural gas price
P_{MT}	Electricity energy produced by MT	η_{MT}	Efficiency of MT
Δt	Dispatch interval time	Q_{MT}	Residual heat of exhaust air
η_l	Heat loss factor of CCHP system	Q_H	Heating capacity by exhaust
Q_C	Cooling capacity by exhaust	$\eta_{H.REC}$	Heat efficiency
$\eta_{C.REC}$	Cooling efficiency	ζ_{H,ζ_C}	Heating and refrigeration coefficient
SB	Storage battery	LCQ	Load control quantity
OMC	Operation and maintenance cost	LCC	Load control compensation
$F_1(t)$	OMC of the whole MG	$F_2(t)$	Pollutant disposal cost
$F_3(t)$	LCC of MG	P_i^t	Generation output of micro source i
$C_i(P_i^t)$	Fuel cost of micro source i	K_i	Maintenance factor of micro source i
K_H	Maintenance factor of HES module	K_C	Maintenance factor of AC modules
P_H^t	Heat power generated by HES	P_C^t	Cooling power generated by AC

E_{ik}	Released quantity of pollutant k	N	The number of generation units
M	The number of pollutant types	α_k	Conversion coefficient for pollutant
EENS	Expected energy not supplied	UIC	Unit interruption cost
p_D^t	The UIC of MG	P_{cut}^t	The LCQ of MG
P_i	Output of generation unit i	P_L	The electric load demand
P_{cut}	The load control power	Q_{HL}, Q_{CL}	Thermal and cooling load demand
Q_H, Q_C	Supplied thermal and cooling power	P_{min}	Minimum output of generation unit i
$P_{i,max}$	Maximum output of generation unit i	R_{up}, R_{down}	Ramp up/down rate of micro source i
P_i^t	Output of micro source i at time t	P_i^{t-1}	Output of micro source i at time $t-1$
$S_{SOC,min}$	Minimum SOC for battery	$S_{SOC,max}$	Maximum SOC of battery
SOC	State of charge	K_C	Maximum charging proportion
K_D	Maximum discharging proportion	P_{SB}^t	The output power of battery at time t
η_{SBC}, η_{SBD}	The charging/discharging efficiency	Q_B	Capacity of battery
P_{cut}^t	The LCQ in the t -th dispatch interval	$P_{cut,max}$	Load control upper limit of MG
$P_{E,MT}$	The electric output of MT	UPEP	Unified prediction error percentage
$\Delta E\%$	The UPEP of electric load demand	$\Delta H\%$	The UPEP of thermal load demand
$\Delta C\%$	The UPEP of cooling load demand	P_{Re}	Predicted electric load demand
H_{Re}	Predicted thermal load demand	C_{Re}	Predicted cooling load demand
ΔP_E	Difference of actual and predicted EL	ΔH	Difference of actual and predicted TL
ΔC	Difference of actual and predicted CL	ΔP_{PV}	Difference of actual and predicted electric output of PV
ΔP_{WT}	Difference of actual and predicted electric output of WT	ΔP_{MT}	Difference of actual and predicted electric output of MT
K_{ES}, K_{MT}	Maintenance factors of ESS and MT	P_{ES}^t	Charge/discharge quantity of EES
ΔP_{MT}^t	Output adjustments of MT	ΔP_H^t	Predicted error of heat load demand
ΔP_C^t	Predicted error of cooling load demand	$C_{MT}(\Delta P_{MT}^t)$	The fuel cost change of MT
ΔP_{cut}^t	LCQ difference of two time scales	p_{best}	The individual optimal solution
g_{best}	The population optimal solution	w	The inertia weight
c_1, c_2	Learning factors	r_1, r_2	Random numbers between 0 and 1
d	Dimension of the optimization model	p_{ij}	Individual optimal solution
$p_{g,j}$	Population optimal solution	$v_{i,j}(t)$	Velocity vectors for particle i in the j -th dimension at moment t
$v_{i,j}(t+1)$	Velocity vectors for particle i in the j -th dimension at moment $t + 1$	$x_{i,j}(t)$	Position vector for particle i in the j -th dimension at moment t
$x_{i,j}(t+1)$	Position vector for particle i in the j -th dimension at moment $t + 1$	X_i	The i -th solution in the population
X_{best}	The best individual	X_{worst}	The worst individual
X_m, X_n	Selected particles randomly	Δ	Random number between 0 and 1
X^1_{cross}	New particle obtained by cross	X^2_{cross}	New particle obtained by cross
EL	Electric load	TL	Thermal load
CL	Cooling load	MPPT	Maximum power point tracking
OPBH	Ordering power by heat	AQ	Adjustment quantity

References

- Amrollahi, M.H.; Bathaee, S.M.T. Techno-economic optimization of hybrid photovoltaic/wind generation together with energy storage system in a stand-alone micro-grid subjected to demand response. *Appl. Energy* **2017**, *202*, 66–77. [[CrossRef](#)]
- Craparo, E.; Karatas, M.; Singham, D.I.; Fan, W.; Liu, J. A robust optimization approach to hybrid microgrid operation using ensemble weather forecasts. *Appl. Energy* **2017**, *201*, 135–147. [[CrossRef](#)]
- Huang, C.; Yue, D.; Deng, S.; Xie, J. Optimal Scheduling of Microgrid with Multiple Distributed Resources Using Interval Optimization. *Energies* **2017**, *10*, 339. [[CrossRef](#)]
- Ackermann, T.; Andersson, G.; Söder, L. Distributed generation: A definition. *Electr. Power Syst. Res.* **2001**, *57*, 195–204. [[CrossRef](#)]
- Hashemi, F.; Mohammadi, M.; Kargarian, A. Islanding detection method for microgrid based on extracted features from differential transient rate of change of frequency. *IET Gener. Transm. Distrib.* **2017**, *11*, 891–904. [[CrossRef](#)]
- Ou, T.-C. A novel unsymmetrical faults analysis for microgrid distribution systems. *Int. J. Electr. Power Energy Syst.* **2012**, *43*, 1017–1024. [[CrossRef](#)]
- Ou, T.; Lu, K.; Huang, C. Improvement of Transient Stability in a Hybrid Power Multi-System Using a Designed NIDC (Novel Intelligent Damping Controller). *Energies* **2017**, *10*, 488. [[CrossRef](#)]

8. Ou, T.-C. Ground fault current analysis with a direct building algorithm for microgrid distribution. *Int. J. Electr. Power Energy Syst.* **2013**, *53*, 867–875. [[CrossRef](#)]
9. Bustos, C.; Watts, D. Novel methodology for microgrids in isolated communities: Electricity cost-coverage trade-off with 3-stage technology mix, dispatch & configuration optimizations. *Appl. Energy* **2017**, *195*, 204–221.
10. Wang, C.; Liu, Y.; Li, X.; Guo, L.; Qiao, L.; Lu, H. Energy management system for stand-alone diesel-wind-biomass microgrid with energy storage system. *Energy* **2016**, *97*, 90–104. [[CrossRef](#)]
11. Ou, T.; Su, W.; Liu, X.; Huang, S.; Tai, T. A Modified Bird-Mating Optimization with Hill-Climbing for Connection Decisions of Transformers. *Energies* **2016**, *9*, 671. [[CrossRef](#)]
12. Ali, M.H. *Wind Energy Systems: Solutions for Power Quality and Stabilization*; CRC Press–Taylor & Francis Group: Boca Raton, FL, USA, 2012.
13. Ghasemi, A. Coordination of pumped-storage unit and irrigation system with intermittent wind generation for intelligent energy management of an agricultural microgrid. *Energy* **2018**, *142*, 1–13. [[CrossRef](#)]
14. Ou, T.-C.; Hong, C.-M. Dynamic operation and control of microgrid hybrid power systems. *Energy* **2014**, *66*, 314–323. [[CrossRef](#)]
15. Mohseni, A.; Mortazavi, S.S.; Ghasemi, A.; Nahavandi, A.; abdi, M.T. The application of household appliances' flexibility by set of sequential uninterruptible energy phases model in the day-ahead planning of a residential microgrid. *Energy* **2017**, *139*, 315–328. [[CrossRef](#)]
16. Sachs, J.; Sawodny, O. Multi-objective three stage design optimization for island microgrids. *Appl. Energy* **2016**, *165*, 789–800. [[CrossRef](#)]
17. Wang, F.; Zhen, Z.; Mi, Z.; Sun, H.; Su, S.; Yang, G. Solar irradiance feature extraction and support vector machines based weather status pattern recognition model for short-term photovoltaic power forecasting. *Energy Build.* **2015**, *86*, 427–438. [[CrossRef](#)]
18. Chen, Q.; Wang, F.; Hodge, B.M.; Zhang, J.; Li, Z.; Shafie-khah, M.; Catalão, J.P.S. Dynamic price vector formation model based automatic demand response strategy for PV-assisted EV charging station. *IEEE Trans. Smart Grid.* **2017**, *8*, 2903–2915. [[CrossRef](#)]
19. Wang, F.; Mi, Z.; Su, S.; Zhao, H. Short-Term Solar Irradiance Forecasting Model Based on Artificial Neural Network Using Statistical Feature Parameters. *Energies* **2012**, *5*, 1355–1370. [[CrossRef](#)]
20. Silvente, J.; Kopanos, G.M.; Pistikopoulos, E.N.; Espuña, A. A rolling horizon optimization framework for the simultaneous energy supply and demand planning in microgrids. *Appl. Energy* **2015**, *155*, 485–501. [[CrossRef](#)]
21. Di Piazza, M.C.; La Tona, G.; Luna, M.; Di Piazza, A. A two-stage Energy Management System for smart buildings reducing the impact of demand uncertainty. *Energy Build.* **2017**, *139*, 1–9. [[CrossRef](#)]
22. Korkas, C.D.; Baldi, S.; Michailidis, I.; Kosmatopoulos, E.B. Occupancy-based demand response and thermal comfort optimization in microgrids with renewable energy sources and energy storage. *Appl. Energy* **2016**, *163*, 93–104. [[CrossRef](#)]
23. Guo, L.; Liu, W.; Jiao, B.; Hong, B.; Wang, C. Multi-objective stochastic optimal planning method for stand-alone microgrid system. *IET Gener. Transm. Distrib.* **2014**, *8*, 1263–1273. [[CrossRef](#)]
24. Li, P.; Xu, D.; Zhou, Z.; Lee, W.J.; Zhao, B. Stochastic Optimal Operation of Microgrid Based on Chaotic Binary Particle Swarm Optimization. *IEEE Trans. Smart Grid* **2016**, *7*, 66–73. [[CrossRef](#)]
25. Talari, S.; Yazdaninejad, M.; Haghifam, M.R. Stochastic-based scheduling of the microgrid operation including wind turbines, photovoltaic cells, energy storages and responsive loads. *IET Gener. Transm. Distrib.* **2015**, *9*, 1498–1509. [[CrossRef](#)]
26. Wang, F.; Xu, H.; Xu, T.; Li, K.; Shafie-khah, M.; Catalão, J.P.S. The values of market-based demand response on improving power system reliability under extreme circumstances. *Appl. Energy* **2017**, *193*, 220–231. [[CrossRef](#)]
27. Paterakis, N.G.; Erdinç, O.; Catalão, J.P.S. An overview of Demand Response: Key-elements and international experience. *Renew. Sustain. Energy Rev.* **2017**, *69*, 871–891. [[CrossRef](#)]
28. Erdinc, O.; Paterakis, N.G.; Pappi, I.N.; Bakirtzis, A.G.; Catalão, J.P.S. A new perspective for sizing of distributed generation and energy storage for smart households under demand response. *Appl. Energy* **2015**, *143*, 26–37. [[CrossRef](#)]
29. Pina, A.; Silva, C.; Ferrão, P. The impact of demand side management strategies in the penetration of renewable electricity. *Energy* **2012**, *41*, 128–137. [[CrossRef](#)]

30. Neves, D.; Silva, C.A. Optimal electricity dispatch on isolated mini-grids using a demand response strategy for thermal storage backup with genetic algorithms. *Energy* **2015**, *82*, 436–445. [[CrossRef](#)]
31. Zakariazadeh, A.; Jadid, S.; Siano, P. Smart microgrid energy and reserve scheduling with demand response using stochastic optimization. *Int. J. Electr. Power Energy Syst.* **2014**, *63*, 523–533. [[CrossRef](#)]
32. Carpinelli, G.; Mottola, F.; Proto, D. Optimal scheduling of a microgrid with demand response resources. *IET Gener. Transm. Distrib.* **2014**, *8*, 1891–1899. [[CrossRef](#)]
33. Gelazanskas, L.; Gamage, K.A.A. Demand side management in smart grid: A review and proposals for future direction. *Sustain. Cities Soc.* **2014**, *11*, 22–30. [[CrossRef](#)]
34. Livengood, D.; Larson, R. The energy box: Locally automated optimal control of residential electricity usage. *Serv. Sci.* **2009**, *1*, 1–16. [[CrossRef](#)]
35. Moradi, H.; Esfahanian, M.; Abtahi, A.; Zilouchian, A. Modeling a Hybrid Microgrid Using Probabilistic Reconfiguration under System Uncertainties. *Energies* **2017**, *10*, 1430. [[CrossRef](#)]
36. Nazari-Heris, M.; Abapour, S.; Mohammadi-Ivatloo, B. Optimal economic dispatch of FC-CHP based heat and power micro-grids. *Appl. Therm. Eng.* **2017**, *114*, 756–769. [[CrossRef](#)]
37. Farzin, H.; Fotuhi-Firuzabad, M.; Moeini-Agtaie, M. A Stochastic Multi-Objective Framework for Optimal Scheduling of Energy Storage Systems in Microgrids. *IEEE Trans. Smart Grid* **2017**, *8*, 117–127. [[CrossRef](#)]
38. Kerdphol, T.; Fuji, K.; Mitani, Y.; Watanabe, M.; Qudaih, Y. Optimization of a battery energy storage system using particle swarm optimization for stand-alone microgrids. *Int. J. Electr. Power Energy Syst.* **2016**, *81*, 32–39. [[CrossRef](#)]
39. Pedrasa, M.A.A.; Spooner, T.D.; MacGill, I.F. Scheduling of demand side resources using binary particle swarm optimization. *IEEE Trans. Power Syst.* **2009**, *24*, 1173–1181. [[CrossRef](#)]
40. You, M.; Jiang, T. New method for target identification in a foliage environment using selected bispectra and chaos particle swarm optimization based support vector machine. *IET Signal Process.* **2014**, *8*, 76–84. [[CrossRef](#)]
41. Ahn, C.W.; Ramakrishna, R.S. Elitism-based compact genetic algorithms. *IEEE Trans. Evolut. Comput.* **2003**, *7*, 367–385.
42. Waqar, A.; Shahbaz Tanveer, M.; Ahmad, J.; Aamir, M.; Yaqoob, M.; Anwar, F. Multi-Objective Analysis of a CHP Plant Integrated Microgrid in Pakistan. *Energies* **2017**, *10*, 1625. [[CrossRef](#)]
43. Martinez, A.A.; Champenois, G. Eco-design optimisation of an autonomous hybrid wind-photovoltaic system with battery storage. *IET Renew. Power Gener.* **2012**, *6*, 358–371.
44. Azmy, A.M.; Erlich, I. Online optimal management of PEMFuel cells using neural networks. *IEEE Trans. Power Deliv.* **2005**, *20*, 1051–1058. [[CrossRef](#)]
45. Noroozian, R.; Vahedi, H. Optimal management of MicroGrid using Bacterial Foraging Algorithm. In Proceedings of the 2010 18th Iranian Conference on Electrical Engineering, Isfahan, Iran, 11–13 May 2010; pp. 895–900.
46. Nguyen, T.A.; Crow, M.L.; Elmore, A.C. Optimal Sizing of a Vanadium Redox Battery System for Microgrid Systems. *IEEE Trans. Sustain. Energy* **2015**, *6*, 729–737. [[CrossRef](#)]
47. Mohamed, F.A.; Koivo, H.N. System modelling and online optimal management of MicroGrid using Mesh Adaptive Direct Search. *Int. J. Electr. Power Energy Syst.* **2010**, *32*, 398–407. [[CrossRef](#)]
48. Parisio, A.; Rikos, E.; Tzamalis, G.; Glielmo, L. Use of model predictive control for experimental microgrid optimization. *Appl. Energy* **2014**, *115*, 37–46. [[CrossRef](#)]
49. Delgarm, N.; Sajadi, B.; Kowsary, F.; Delgarm, S. Multi-objective optimization of the building energy performance: A simulation-based approach by means of particle swarm optimization (PSO). *Appl. Energy* **2016**, *170*, 293–303. [[CrossRef](#)]
50. Sadeghzadeh, H.; Ehyaei, M.A.; Rosen, M.A. Techno-economic optimization of a shell and tube heat exchanger by genetic and particle swarm algorithms. *Energy Convers. Manag.* **2015**, *93*, 84–91. [[CrossRef](#)]
51. Tang, J.; Wang, D.; Wang, X.; Jia, H.; Wang, C.; Huang, R.; Yang, Z.; Fan, M. Study on day-ahead optimal economic operation of active distribution networks based on Kriging model assisted particle swarm optimization with constraint handling techniques. *Appl. Energy* **2017**, *204*, 143–162. [[CrossRef](#)]
52. Mohammadi, S.; Mozafari, B.; Solimani, S.; Niknam, T. An Adaptive Modified Firefly Optimisation Algorithm based on Hong's Point Estimate Method to optimal operation management in a microgrid with consideration of uncertainties. *Energy* **2013**, *51*, 339–348. [[CrossRef](#)]

53. Zhou, Q.; Zhang, W.; Cash, S.; Olatunbosun, O.; Xu, H.; Lu, G. Intelligent sizing of a series hybrid electric power-train system based on Chaos-enhanced accelerated particle swarm optimization. *Appl. Energy* **2017**, *189*, 588–601. [[CrossRef](#)]
54. Diaf, S.; Diaf, D.; Belhamel, M.; Haddadi, M.; Louche, A. A methodology for optimal sizing of autonomous hybrid PV/wind system. *Energy Policy* **2007**, *35*, 5708–5718. [[CrossRef](#)]
55. Pipattanasomporn, M.; Willingham, M.; Rahman, S. Implications of on-site distributed generation for commercial/industrial facilities. *IEEE Trans. Power Syst.* **2005**, *20*, 206–212. [[CrossRef](#)]
56. Bernow, S.; Marron, D. *Valuation of Environmental Externalities for Energy Planning and Operations*; Tellus Institute Report 90-SB01; Tellus Institute: Boston, MA, USA, 1990.



© 2017 by the authors. Licensee MDPI, Basel, Switzerland. This article is an open access article distributed under the terms and conditions of the Creative Commons Attribution (CC BY) license (<http://creativecommons.org/licenses/by/4.0/>).